

## Supplementary Material

### Catalytic enrichment of plasma with hydroxyl radicals in aqueous phase at room temperature

Maïté Audemar<sup>1</sup>, Oriol Vallcorba<sup>2</sup>, Inma Peral<sup>3</sup>, Jean-Sébastien Thomann<sup>4</sup>, Agata Przekora<sup>5</sup>,  
Joanna Pawlat<sup>6</sup>, Cristina Canal<sup>7,8,9</sup>, Grazyna Ginalska<sup>5</sup>, Michał Kwiatkowski<sup>6</sup>, David Duday<sup>4</sup> and  
Sophie Hermans<sup>1</sup>

### Table of Contents

Figure S1: Nitrogen adsorption/desorption isotherms at 77 K of the synthesized MCM-48 material and (inset) DFT pore size distribution obtained from N<sub>2</sub> physisorption (adsorption)

Figure S2: TEM image and size distribution of hydrophobic Fe<sub>3</sub>O<sub>4</sub>(o) nanoparticles

Figure S3: XRD diffractogram of hydrophobic Fe<sub>3</sub>O<sub>4</sub>(o) nanoparticles

Figure S4: XRD patterns of the Fe<sub>3</sub>O<sub>4</sub>(o)/MCM-48(FI) and Fe<sub>3</sub>O<sub>4</sub>(i)/MCM-48(FI) catalysts prepared by ferrofluids impregnation (Bump at 63-64° due to the instrument)

Figure S5: (a) Nitrogen physisorption isotherms at 77 K of the synthesized MCM-48 and the Fe<sub>3</sub>O<sub>4</sub>/MCM-48(CP) catalyst and (b) DFT pore size distribution obtained from N<sub>2</sub> physisorption (adsorption). Specific surface area: MCM-48 = 1440 m<sup>2</sup>/g, Fe<sub>3</sub>O<sub>4</sub>/MCM-48(copre) = 555 m<sup>2</sup>/g

Figure S6: XRD patterns of (a) the Fe<sub>x</sub>O<sub>y</sub>/MCM-48(I) and Fe<sub>x</sub>O<sub>y</sub>/MCM-48(I-EtOH) catalysts and (b) the Fe<sub>x</sub>O<sub>y</sub>/MNPs(I-EtOH) catalyst obtained by dry impregnation and activated at 500 °C (Bump at 63-64° due to the instrument)

Figure S7: XRD patterns of (a) Fe<sub>x</sub>O<sub>y</sub>/MCM-48(I-EtOH) and (b) Fe<sub>x</sub>O<sub>y</sub>/MNPs(I-EtOH) catalysts after catalytic tests in milliQ water and acidic solution

Figure S8: Temperature Programmed Reduction (TPR) profile of the catalyst Fe<sub>x</sub>O<sub>y</sub>/MCM-48(I) obtained by dry impregnation (a) in aqueous solution and (b) in ethanolic solution

Figure S9: (a) Nitrogen adsorption/desorption isotherms at 77 K of the synthesized MSNPs material and (b) pore size distribution (desorption)

Figure S2: (A) SEM image of the MSNPs and (B) hydrodynamic diameter of MSNPs particles in milliQ water by NTA (a no significant peak is observed at 250 nm, possibly resulting from an impurity in the analyzed solution)

Figure S3: (a) TEM image and (b) SEM-EDX mapping of Si, Fe, O components in Fe<sub>x</sub>O<sub>y</sub>/MSNPs(I-EtOH) sample and (c) in Fe<sub>x</sub>O<sub>y</sub>/MCM-48(I-EtOH) sample

Figure S4: TGA in air and DSC characterization of the surface modified Fe<sub>3</sub>O<sub>4</sub>-Br NPs and surface modified MCM-48 samples

Figure S5: Fluorescence intensity at various reaction times for the catalytic production of HO• radicals with the hydrophilic Fe<sub>3</sub>O<sub>4</sub>(i) nanoparticles (unsupported)

Figure S14: Umbelliferone evolution during the reaction with the  $\text{Fe}_x\text{O}_y/\text{MCM-48}(\text{I-EtOH})$  and the  $\text{Fe}_x\text{O}_y/\text{MSNPs}(\text{I-EtOH})$  catalysts in acidic conditions with (light green and blue) or without plasma treatment (dark green)

Figure S7: Comparison between the results obtained with the  $\text{Fe}_x\text{O}_y/\text{MSNPs}(\text{I-EtOH})$  catalyst without plasma, and the curve 'difference' obtained by subtraction of the results for the plasma alone from the results plasma +  $\text{Fe}_x\text{O}_y/\text{MSNPs}(\text{I-EtOH})$

Table S1: Iron leaching values during catalytic tests, measured by ICP analysis of the solutions

Table S2: XPS results (at.%) for the  $\text{Fe}_x\text{O}_y/\text{MCM-48}(\text{I-EtOH})$  and  $\text{Fe}_x\text{O}_y/\text{MNPs}(\text{I-EtOH})$  catalysts after catalytic test in milliQ water or acidic solution

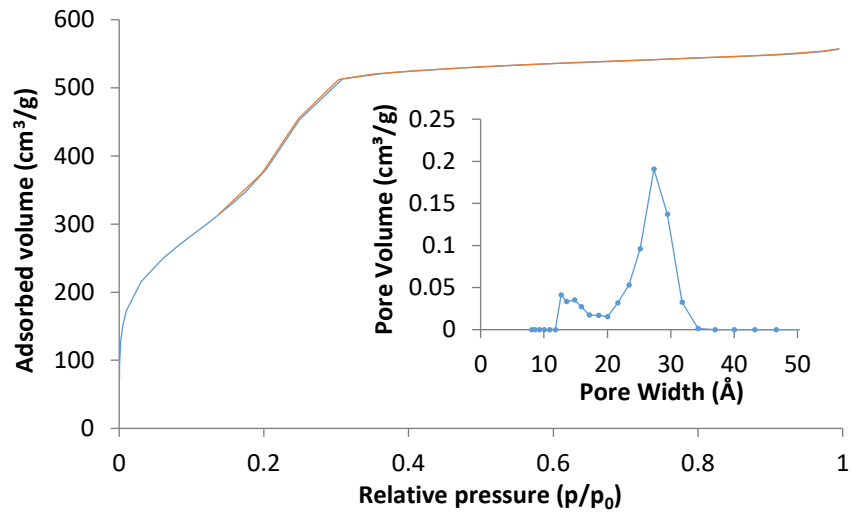


Figure S1: Nitrogen adsorption/desorption isotherms at 77 K of the synthesized MCM-48 material and (inset) DFT pore size distribution obtained from N<sub>2</sub> physisorption (adsorption)

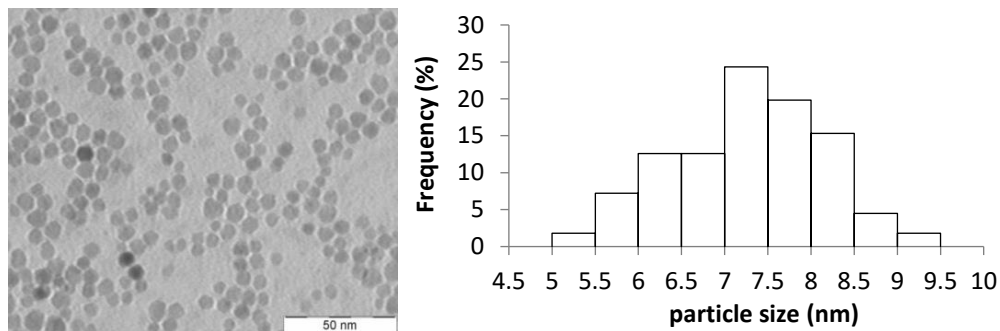


Figure S2: TEM image and size distribution of hydrophobic Fe<sub>3</sub>O<sub>4</sub>(o) nanoparticles

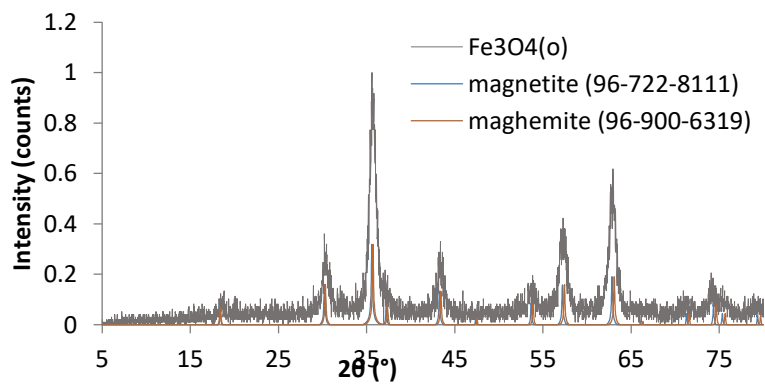


Figure S3: XRD diffractogram of hydrophobic Fe<sub>3</sub>O<sub>4</sub>(o) nanoparticles

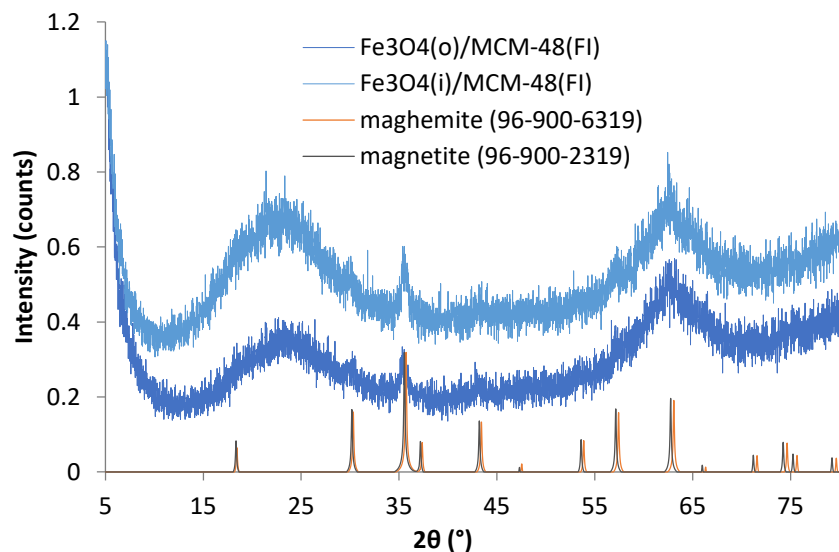


Figure S4: XRD patterns of the Fe<sub>3</sub>O<sub>4</sub>(o)/MCM-48(FI) and Fe<sub>3</sub>O<sub>4</sub>(i)/MCM-48(FI) catalysts prepared by ferrofluids impregnation (Bump at 63-64° due to the instrument) and reference data for maghemite and magnetite phases

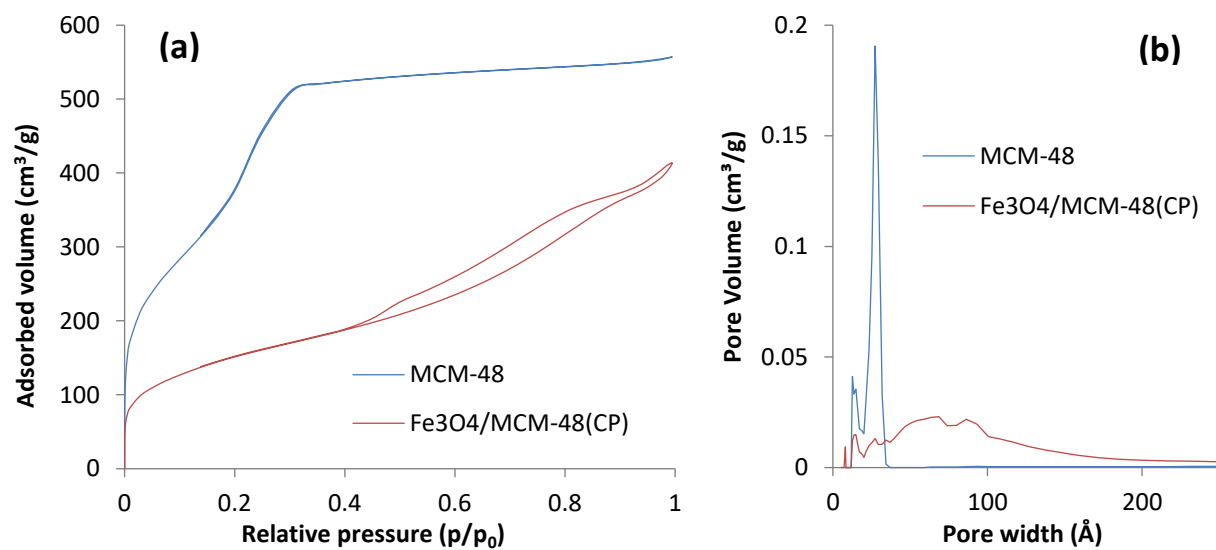


Figure S5: (a) Nitrogen physisorption isotherms at 77 K of the synthesized MCM-48 and the Fe<sub>3</sub>O<sub>4</sub>/MCM-48(CP) catalyst and (b) DFT pore size distribution obtained from N<sub>2</sub> physisorption (adsorption). Specific surface area: MCM-48 = 1440 m<sup>2</sup>/g, Fe<sub>3</sub>O<sub>4</sub>/MCM-48(copre) = 555 m<sup>2</sup>/g

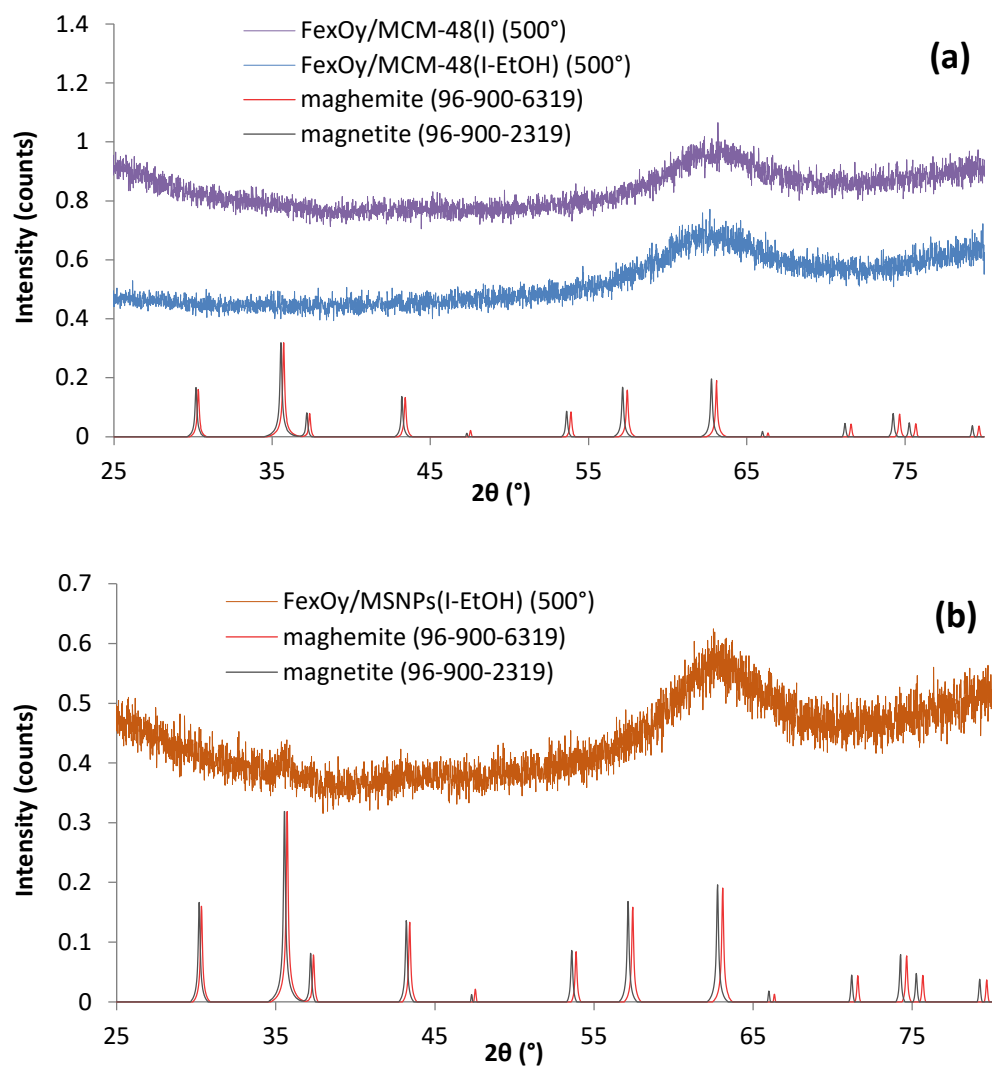


Figure S6: XRD patterns of (a) the Fe<sub>x</sub>O<sub>y</sub>/MCM-48(I) and Fe<sub>x</sub>O<sub>y</sub>/MCM-48(I-EtOH) catalysts and (b) the Fe<sub>x</sub>O<sub>y</sub>/MNPs(I-EtOH) catalyst obtained by dry impregnation and activated at 500 °C (Bump at 63-64° due to the instrument) and reference data for maghemite and magnetite phases

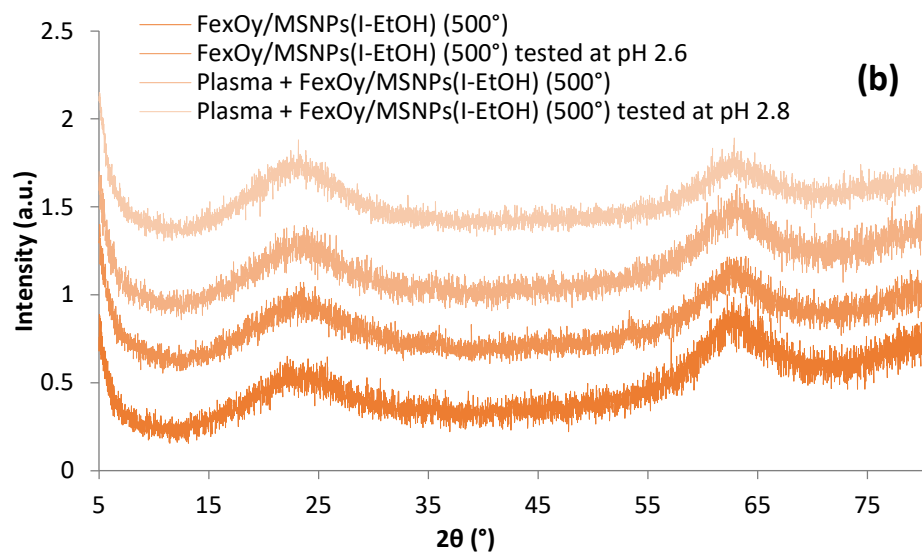
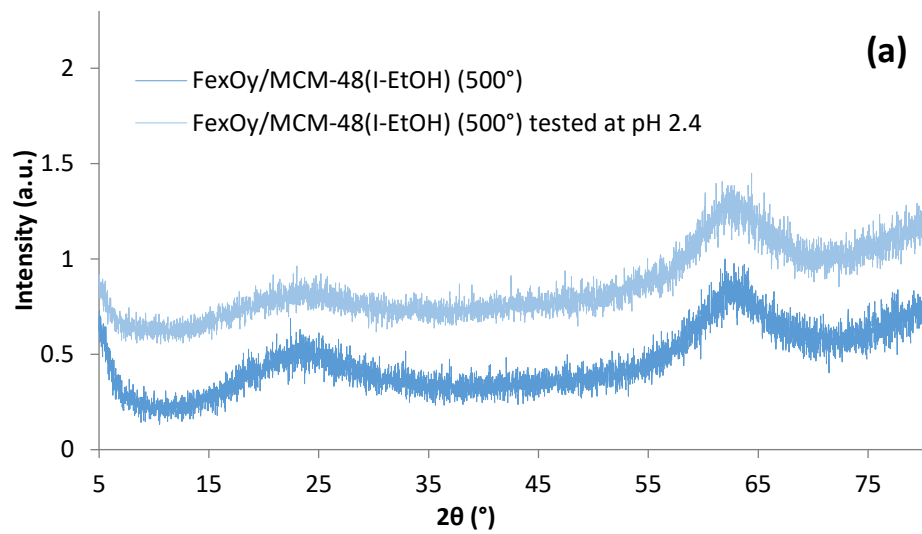


Figure S7: XRD patterns of (a) Fe<sub>3</sub>O<sub>4</sub>/MCM-48(I-EtOH) and (b) Fe<sub>3</sub>O<sub>4</sub>/MNP(I-EtOH) catalysts after catalytic tests in milliQ water and acidic solution

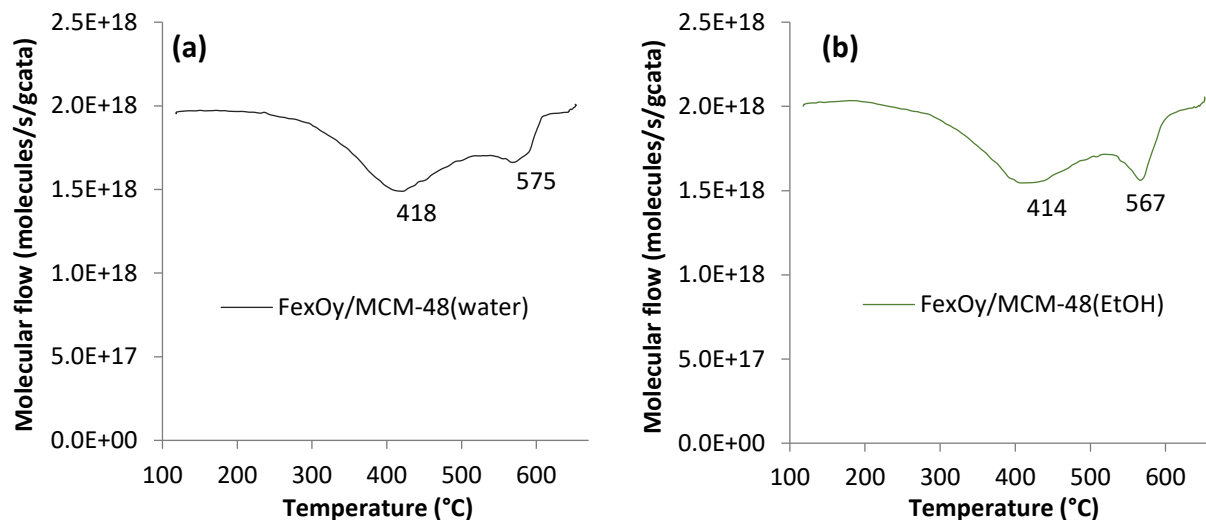


Figure S8: Temperature Programmed Reduction (TPR) profile of the catalyst Fe<sub>x</sub>O<sub>y</sub>/MCM-48(I) obtained by dry impregnation (a) in aqueous solution and (b) in ethanolic solution

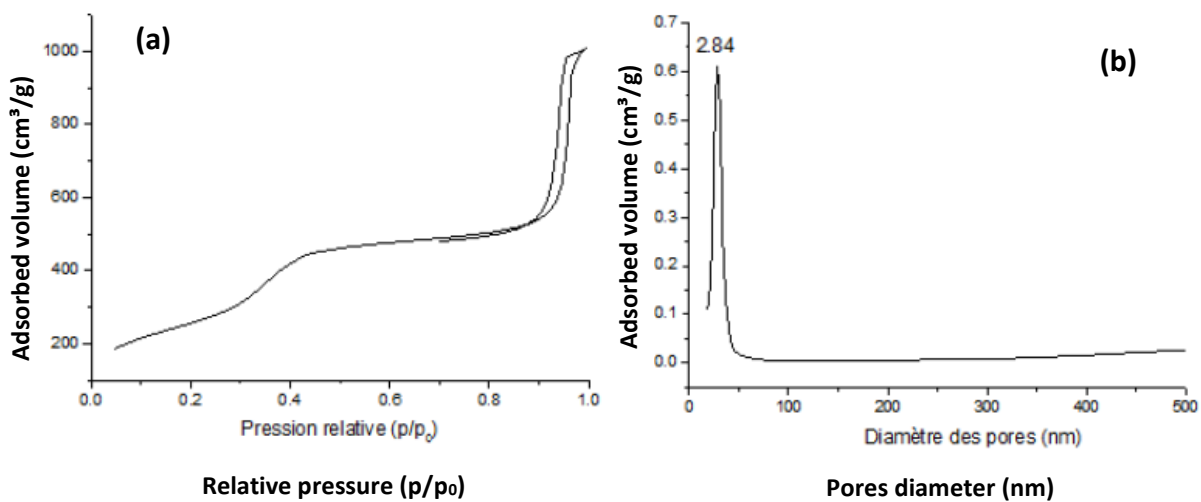


Figure S9: (a) Nitrogen adsorption/desorption isotherms at 77 K of the synthesized MSNPs material and (b) pore size distribution (desorption)

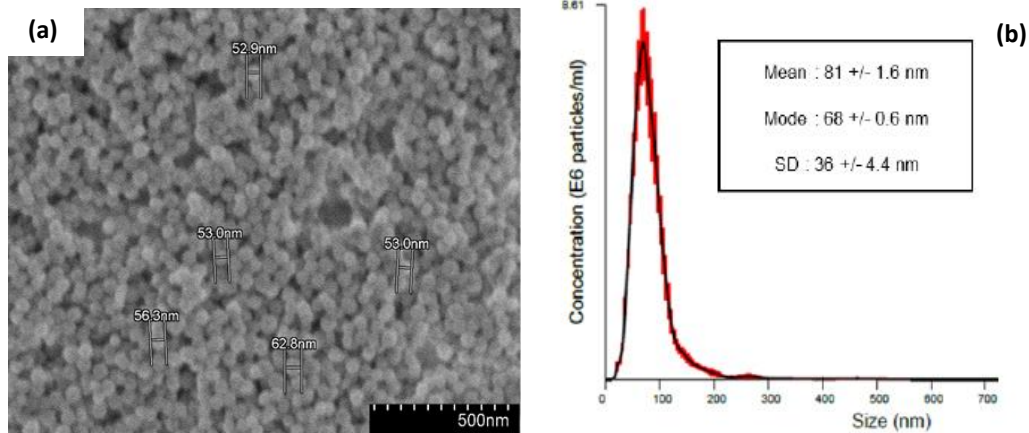


Figure S2: (A) SEM image of the MSNPs and (B) hydrodynamic diameter of MSNPs particles in milliQ water by NTA (a no significant peak is observed at 250 nm, possibly resulting from an impurity in the analyzed solution)

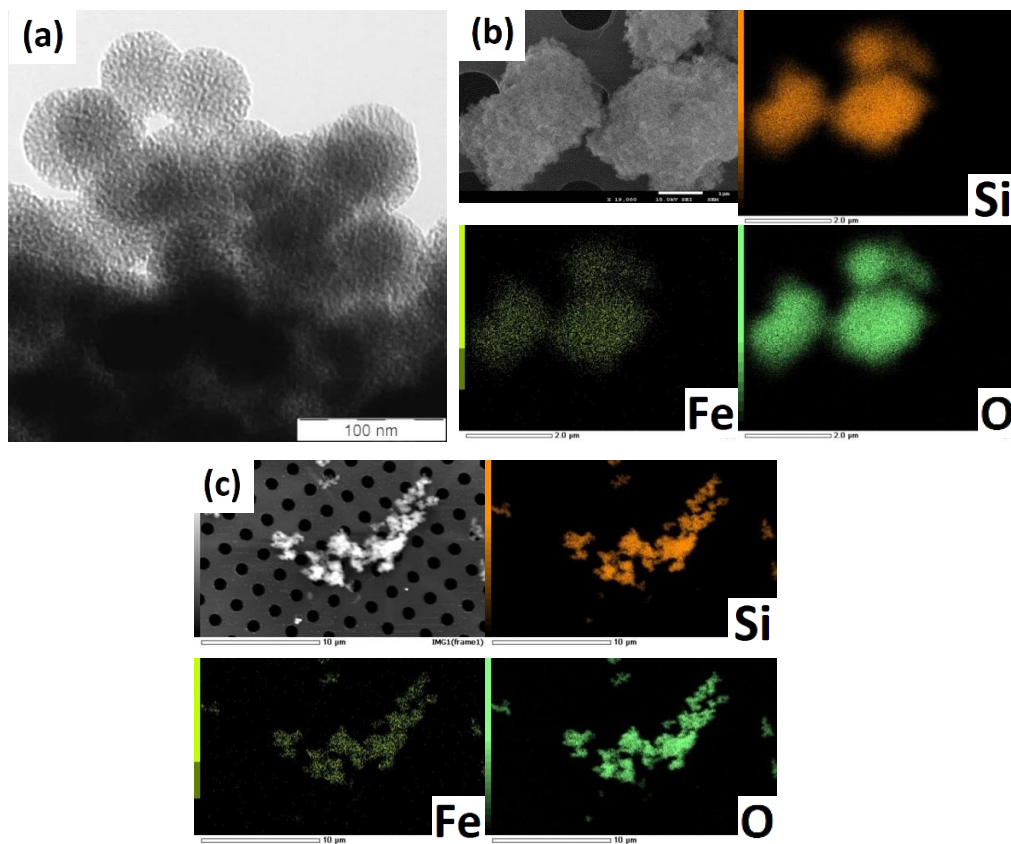


Figure S3: (a) TEM image and (b) SEM-EDX mapping of Si, Fe, O components in Fe<sub>x</sub>O<sub>y</sub>/MSNPs(I-EtOH) sample and (c) in Fe<sub>x</sub>O<sub>y</sub>/MCM-48(I-EtOH) sample



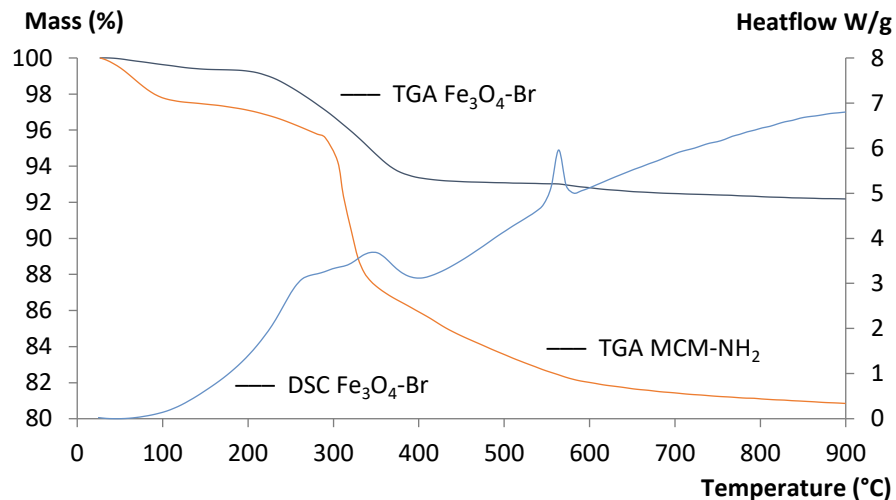


Figure S4: TGA in air and DSC characterization of the surface modified Fe<sub>3</sub>O<sub>4</sub>-Br NPs and surface modified MCM-48 samples

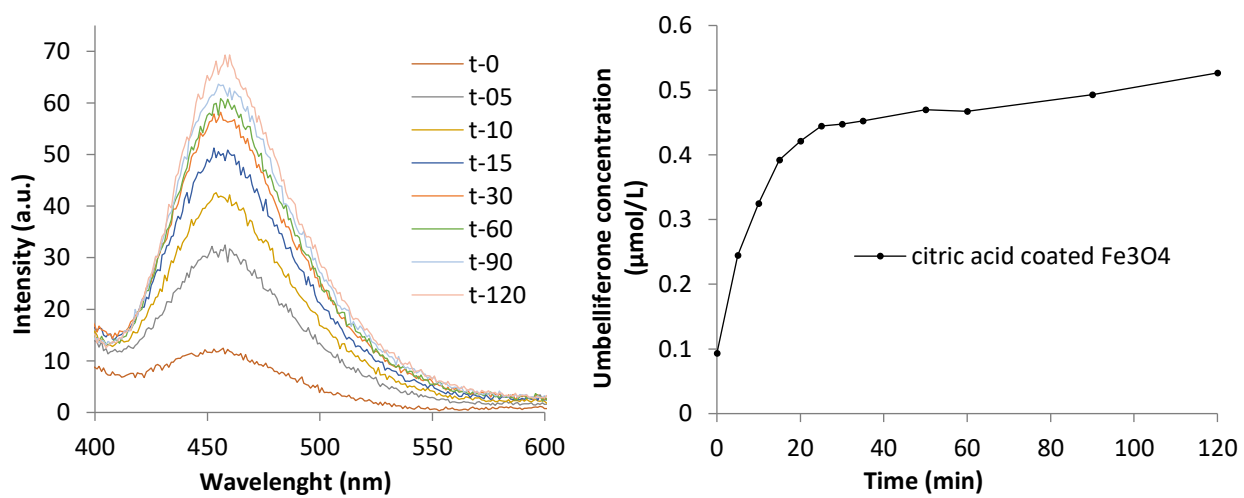


Figure S5: Fluorescence intensity at various reaction times for the catalytic production of HO<sup>•</sup> radicals with the hydrophilic Fe<sub>3</sub>O<sub>4</sub>(i) nanoparticles (unsupported)

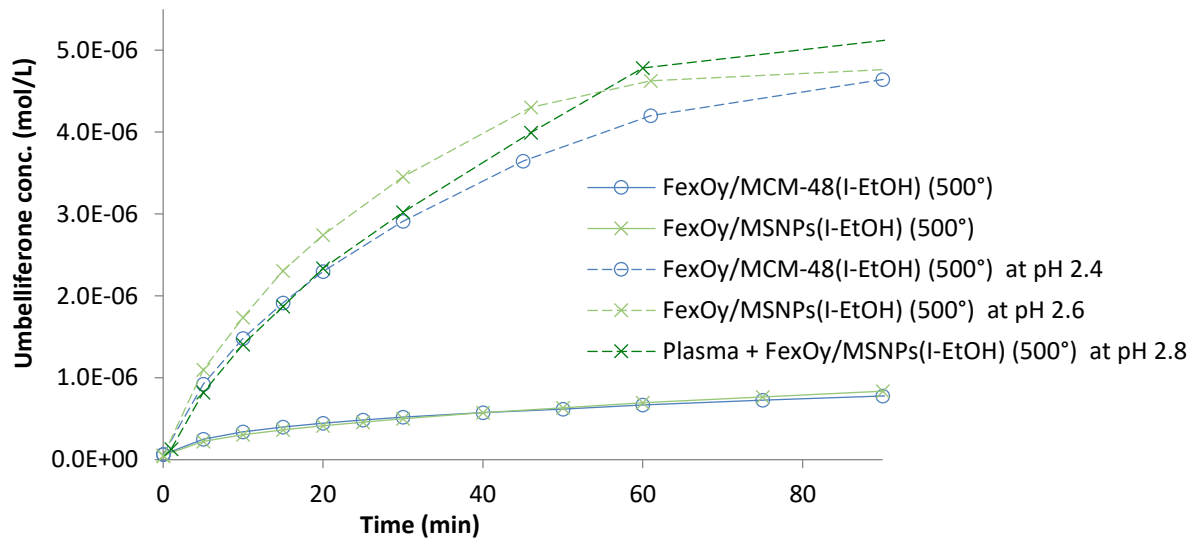


Figure S6: Umbelliferone evolution during the reaction with the  $\text{Fe}_x\text{O}_y/\text{MCM-48(I-EtOH)}$  and the  $\text{Fe}_x\text{O}_y/\text{MSNPs(I-EtOH)}$  catalysts in acidic conditions with (light green and blue) or without plasma treatment (dark green)

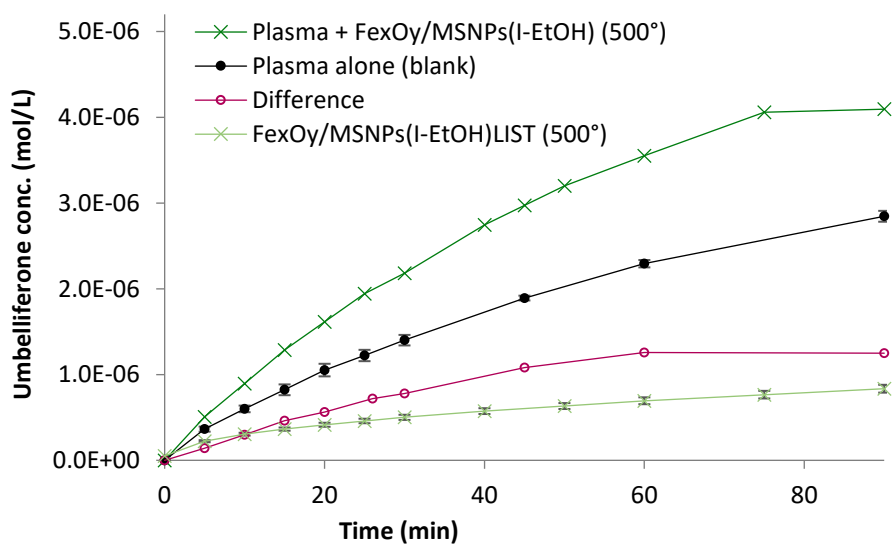


Figure S7: Comparison between the results obtained with the  $\text{Fe}_x\text{O}_y/\text{MSNPs(I-EtOH)}$  catalyst without plasma, and the curve 'difference' obtained by subtraction of the results for the plasma alone from the results plasma +  $\text{Fe}_x\text{O}_y/\text{MSNPs(I-EtOH)}$

**Table S3: Iron leaching values during catalytic tests, measured by ICP analysis of the solutions**

Catalysts	Without Plasma		With Plasma irradiation	
	Iron leaching	% tot iron	Iron leaching	% tot iron
Fe <sub>x</sub> O <sub>y</sub> /MCM-48(EtOH)	10 ppb	>0.1 %	8.79 ppm	15 %
Fe <sub>x</sub> O <sub>y</sub> /MSNPs	50 ppb	0.2 %	6.19 ppm	11 %
Fe <sub>x</sub> O <sub>y</sub> /MCM-48(EtOH) at pH 2.4	3.29 ppm	13.2 %	n.d.	n.d.
Fe <sub>x</sub> O <sub>y</sub> /MSNPs at pH 2.6	5.74 ppm	23.0 %	44.66 ppm	78 %

**Table S4: XPS results (at.%) for the Fe<sub>x</sub>O<sub>y</sub>/MCM-48(I-EtOH) and Fe<sub>x</sub>O<sub>y</sub>/MNP(I-EtOH) catalysts after catalytic test in milliQ water or acidic solution**

	Fe <sub>x</sub> O <sub>y</sub> /MCM-48(I-EtOH) after test	Fe <sub>x</sub> O <sub>y</sub> /MCM-48(I-EtOH) after test at pH 2.4	Fe <sub>x</sub> O <sub>y</sub> /MSNPs (I-EtOH) after test	Fe <sub>x</sub> O <sub>y</sub> /MSNPs (I-EtOH) after test at pH 2.6	Plasma + Fe <sub>x</sub> O <sub>y</sub> /MSNPs (I-EtOH) after test	Plasma + Fe <sub>x</sub> O <sub>y</sub> /MSNPs (I-EtOH) after test at pH 2.8
O 1s	68.91	68.72	67.25	66.66	67.33	67.85
Si 2p	26.86	27.92	29.88	31.20	24.86	26.65
O/Si	2.57	2.46	2.25	2.14	2.71	2.55
Fe 2p3	0.54	0.32	0.38	0.26	0.38	0.18
Fe/Si	0.02	0.01	0.01	0.01	0.02	0.01
C 1s	3.68	3.04	2.49	1.88	7.42	5.32